LETTER

doi:10.1038/nature25788

Hierarchical roles of mitochondrial Papi and Zucchini in *Bombyx* germline piRNA biogenesis

Kazumichi M. Nishida[1]*, Kazuhiro Sakakibara[1]*, Yuka W. Iwasaki[2], Hiromi Yamada[1], Ryo Murakami[1], Yukiko Murota[1], Takeshi Kawamura[3,4], Tatsuhiko Kodama[4], Haruhiko Siomi[2] & Mikiko C. Siomi[1]

PIWI-interacting RNAs (piRNAs) are small regulatory RNAs that bind to PIWI proteins to control transposons and maintain genome integrity in animal germ lines[1–3]. piRNA 3′ end formation in the silkworm *Bombyx mori* has been shown to be mediated by the 3′-to-5′ exonuclease Trimmer (Trim; known as PNLDC1 in mammals)[4], and piRNA intermediates are bound with PIWI anchored onto mitochondrial Tudor domain protein Papi[5]. However, it remains unclear whether the Zucchini (Zuc) endonuclease and Nibbler (Nbr) 3′-to-5′ exonuclease, both of which have pivotal roles in piRNA biogenesis in *Drosophila*[6–8], are required for piRNA processing in other species. Here we show that the loss of Zuc in *Bombyx* had no effect on the levels of Trim and Nbr, but resulted in the aberrant accumulation of piRNA intermediates within the Papi complex, and that these were processed to form mature piRNAs by recombinant Zuc. Papi exerted its RNA-binding activity only when bound with PIWI and phosphorylated, suggesting that complex assembly involves a hierarchical process. Both the 5′ and 3′ ends of piRNA intermediates within the Papi complex showed hallmarks of PIWI 'slicer' activity, yet no phasing pattern was observed in mature piRNAs. The loss of Zuc did not affect the 5′- and 3′-end formation of the intermediates, strongly supporting the idea that the 5′ end of *Bombyx* piRNA is formed by PIWI slicer activity, but independently of Zuc, whereas the 3′ end is formed by the Zuc endonuclease. The *Bombyx* piRNA biogenesis machinery is simpler than that of *Drosophila*, because *Bombyx* has no transcriptional silencing machinery that relies on phased piRNAs.

piRNAs are produced through an intricate biogenesis pathway composed of the primary pathway, the amplification loop (also known as the ping-pong cycle), and Zuc-dependent phasing[1–3,6–12]. To understand the mechanism that underlies the amplification machinery, the silkworm ovary-derived, cultured cell line BmN4 has been used[13–15]. BmN4 cells express two PIWI proteins, Siwi and Ago3. Siwi- and Ago3-bound piRNAs show strong nucleotide and strand biases (uracil at position 1 (1U) for the antisense strand, and adenine at position (10A) for the sense strand), and are complementary through 10 nucleotides from their 5′ end, known as the ping-pong signatures[14,15]. Both Siwi and Ago3 are cytoplasmic: that is, silkworms rely on solely post-transcriptional silencing to control transposons, unlike *Drosophila* and mice, which repress transposons both transcriptionally and post-transcriptionally[1–3].

Papi[16] in BmN4 cells is anchored to the surface of mitochondria through a mitochondrial localization signal (MLS), and binds Siwi and Ago3 through their symmetrically dimethylated arginine (sDMA) residues[5]. Depletion of Papi was shown to have little effect on the levels of piRNAs, although piRNAs became several bases longer exclusively at their 3′ end[5]. Trim was identified as the 3′-to-5′ exonuclease required for piRNA 3′ processing in *Bombyx*[4].

Zuc endonuclease is necessary for piRNA biogenesis, particularly for phased piRNA production in *Drosophila* and mice[6–8,17–19]. Nbr exonuclease functions in piRNA 3′-end formation in *Drosophila*[8,20]. The silkworm genome contains homologues of *Zuc* and *Nbr* genes (KAIKObase; http://sgp.dna.affrc.go.jp), both of which are expressed in BmN4 cells (Extended Data Fig. 1a, b). However, loss of Trim and Nbr did not affect the levels of Flag-PIWI-loaded piRNAs, whereas loss of Papi nearly completely abolished the PIWI–piRNA association (Fig. 1a and Extended Data Fig. 1a, c). Papi is essential for piRNA production and formation of the piRNA-induced silencing complex (piRISC) in silkworm germline cells.

PIWI-loaded piRNAs in Trim-depleted cells seemed to be subtly upshifted on RNA gels (Fig. 1a). The mean sizes of Siwi- and Ago3-bound piRNAs were 28.2 and 27.6 nucleotides (in control cells), and 28.6 and 28.2 nucleotides (in Trim-knockdown cells), respectively (Fig. 1b); that is, Siwi- and Ago3-bound piRNAs produced with no Trim function were on average 0.4 and 0.6 nucleotides longer than those in control cells. piRNA sequencing confirmed these results (Extended Data Fig. 2a). The 1U/10A and strand biases were greatly maintained after Trim depletion (Extended Data Fig. 2b, c), suggesting that the changes in piRNA size seem to be attributed to changes at the 3′ end. The population of piRNAs was also barely changed by Trim depletion (Extended Data Fig. 2c). In addition, lack of Nbr caused no notable changes in Siwi- and Ago3-bound piRNAs (Extended Data Fig. 2a–c). Trim may thus act to fine-tune piRNA size at the 3′ end.

piRNAs undergo 2′-*O*-methylation by the methyltransferase Hen1 and become resistant to β-elimination[21,22]. Both Siwi- and Ago3-bound piRNAs, even longer ones, showed firm resistance to β-elimination, regardless of the presence or absence of Trim (Fig. 1c and Extended Data Fig. 3a). It seems that piRNA 2′-*O*-methylation occurs irrespective of Trim depletion. This is at odds with a previous report that claims that the lack of Trim impaired piRNA 3′ end formation, including 2′-*O*-methylation, leading to a severe reduction in the piRNA level in silkworm cells[4].

Mass spectrometric analysis of endogenous PIWI proteins in BmN4 cells revealed that 11 and 5 arginine residues of Siwi and Ago3, respectively, were sDMA-modified (Extended Data Fig. 3b, c and Supplementary Table 1). We substituted 9 out of the 11 arginine residues in Siwi to lysine residues (Siwi-9RK), which completely abolished the Siwi–Papi association (Extended Data Fig. 4a). The Ago3 mutant, which should have lost its sDMA modification, failed to bind Papi, as has been reported previously[5] (Extended Data Fig. 4a). Both mutants were barely loaded with piRNAs (Extended Data Fig. 4b), and failed to accumulate at nuage perinuclear foci[23], the site for germline piRNA biogenesis (Extended Data Fig. 4c). Thus, sDMA modification is essential for the Papi association, nuage localization and piRISC formation of PIWI. Both Siwi and Ago3 were sDMA-modified even after

[1]Department of Biological Sciences, Graduate School of Science, The University of Tokyo, Tokyo 113-0032, Japan. [2]Department of Molecular Biology, Keio University School of Medicine, Tokyo 162-8582, Japan. [3]Proteomics Laboratory, Isotope Science Center, The University of Tokyo, Tokyo 113-0032, Japan. [4]Laboratory for Systems Biology and Medicine, Research Center for Advanced Science and Technology, The University of Tokyo, Tokyo 153-8904, Japan.
*These authors contributed equally to this work.

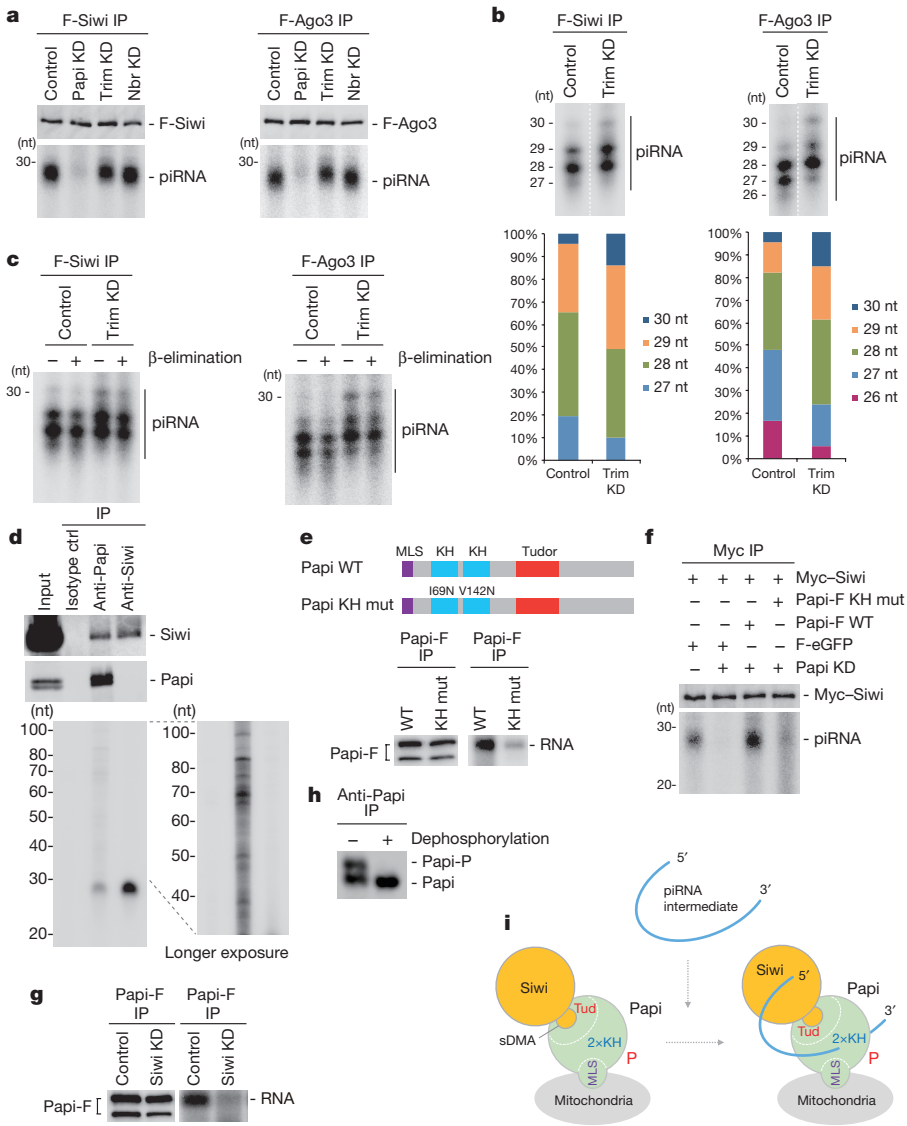

Figure 1 | Papi is essential for piRNA biogenesis and piRISC formation in BmN4 cells. a, Flag-tagged Siwi and Ago3 at the N termini (F-Siwi and F-Ago3, respectively) are loaded with piRNAs in Nbr-knockdown (KD) and Trim-knockdown but not Papi-knockdown BmN4 cells. IP, immunoprecipitation. **b**, piRNAs appear to be slightly longer when Trim is depleted. **c**, β-elimination treatment of Siwi- and Ago3-bound piRNAs from Trim-knockdown and control cells. **d**, RNAs within the Papi complex and bound to Siwi were ^{32}P-labelled at the 5′ end. 'Isotype ctrl' denotes a non-immune IgG antibody. **e**, Wild-type (WT) Papi, but not the KH mutant (mut) Papi, binds to RNAs. Papi-F, Flag-tagged Papi at the C terminus. **f**, Myc–Siwi is unloaded with piRNAs when the KH mutant is expressed in Papi-depleted cells. F-eGFP, Flag-tagged enhanced green fluorescent protein. **g**, Papi does not bind RNAs in Siwi-depleted BmN4 cells. **h**, Papi is phosphorylated (Papi-P) in BmN4 cells. **i**, Model showing that int-piRNA associates with the Papi–Siwi complex on mitochondria. Siwi-sDMA and Papi phosphorylation (P) are required for the assembly. Siwi may be replaced by Ago3 in this model. Tud, Tudor domain.

Papi depletion (Extended Data Fig. 4d), suggesting that the modification occurs before the Papi–PIWI association.

^{32}P-labelling of RNAs within the Papi complex revealed that the levels of mature piRNAs in the complex were approximately 14.6% of those of piRNAs bound to Siwi itself (Fig. 1d), strongly supporting the idea that the piRISC is displaced from Papi after the completion of piRISC formation. The Papi complex contained not only Siwi but also Ago3 as expected, but the level of Ago3 was estimated to be about 10% of that of Siwi in the complex (Extended Data Fig. 5a).

The Papi complex contained RNA molecules longer than piRNAs (Fig. 1d), and this gave a positive result with a northern probe for RT3-1 (Extended Data Fig. 5b). RT3-1 was one of the abundant piRNAs loaded specifically onto Siwi[14]. piRNA intermediates (int-piRNAs) were detected similarly even after Siwi was forcibly displaced from Papi (Extended Data Fig. 5c). The int-piRNAs are therefore physically associated with Siwi in the Papi complex.

Papi contains two KH domains besides the Tudor domain and MLS (Fig. 1e). KH domains are RNA-binding motifs found in RNA-binding proteins that function in various types of RNA metabolism[24]. However, whether Papi exhibits its RNA-binding activity through KH domains has not been examined experimentally. Cross-linking immunoprecipitation (CLIP) experiments showed that Papi–Flag was efficiently cross-linked with RNAs in BmN4 cells, as was endogenous Papi (Fig. 1e and Extended Data Fig. 5d). The Papi–Flag KH mutant, in which Ile69 and Val142 were mutated to asparagine residues, failed to bind RNAs (Fig. 1e). These two residues are highly conserved in KH domain-containing proteins and are crucial for the RNA-binding activity[24]. The Siwi–piRNA association was impeded when the Papi mutant was expressed instead of endogenous Papi (Fig. 1f and Extended Data Fig. 5e). Thus, the RNA-binding activity of Papi through KH domains is essential for piRISC formation.

Not only piRNAs but also int-piRNAs were hardly detected with the Siwi-9RK mutant (Extended Data Fig. 5f). Also, endogenous Siwi in

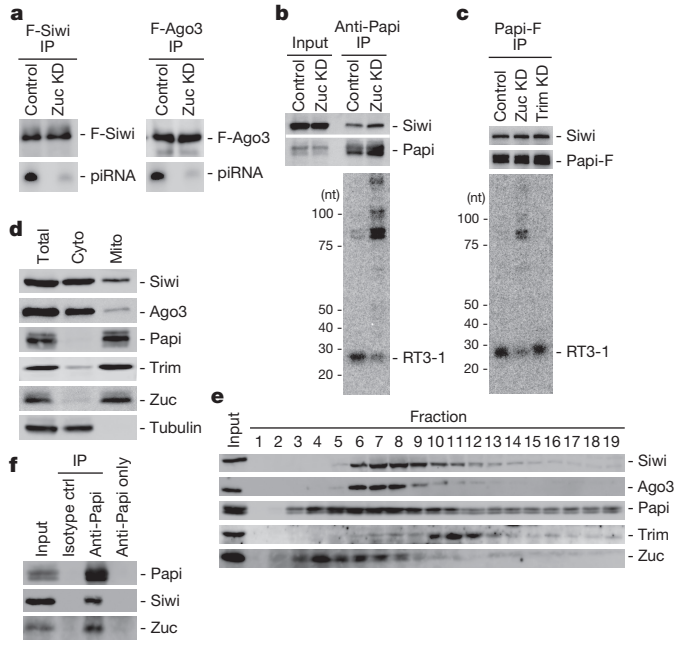

Figure 2 | Zuc is essential for piRNA biogenesis and piRISC formation in BmN4 cells. a, RNAs co-immunoprecipitated with Flag-Siwi and Flag-Ago3 are visualized by ^{32}P labelling. **b**, RT3-1 int-piRNAs aberrantly accumulate in the Papi complex after Zuc depletion. **c**, Trim depletion does not affect the levels of RT3-1 int-piRNAs in the Papi complex. **d**, The presence of endogenous Siwi, Ago3, Papi, Trim and Zuc in the mitochondrial (mito) fraction. Cyto, cytoplasmic fraction. Tubulin was used as a loading control (bottom). **e**, The distribution patterns of endogenous Siwi, Ago3, Papi, Trim and Zuc in mitochondrial fractions 1–19 separated by sucrose gradient sedimentation. Fraction 1 contains the top (lightest) fraction. **f**, Zuc and Siwi are co-immunoprecipitated with Papi from mitochondrial lysates.

Papi-depleted cells was not loaded with either piRNAs or int-piRNAs (Extended Data Fig. 5g). Moreover, the intensity of the Papi CLIP signal decreased markedly when Siwi was depleted (Fig. 1g), although int-piRNAs were detected similarly in total RNAs irrespective of the presence of Siwi (Extended Data Fig. 5h). The Ago3–Papi association should be maintained after Siwi depletion. However, the CLIP signal was very low, agreeing with our earlier notion that the Ago3 level is low in the complex. It is likely that int-piRNAs join the Papi complex only after the Siwi–Papi association.

Both endogenous and exogenous Papi appeared as a doublet but only the top band was cross-linked with RNAs (Fig. 1e, g and Extended Data Fig. 5d). The top band does not represent a splicing variant because ectopically expressed Papi from the full-length cDNA appeared as a doublet. However, Papi became a single band after phosphatase treatment (Fig. 1h). Thus, Papi is subjected to phosphorylation and this modification is essential for it to bind RNAs.

The findings suggest that the assembly of the Papi–PIWI–int-piRNA complex occurs via a hierarchical process (Fig. 1i), which would possibly occur to ensure the funnelling of Siwi–piRNA intermediates to Papi–Siwi and Ago3–piRNA intermediates to the Papi–Ago3 complex. If Papi binds int-piRNA first, there must be a high chance that both Siwi and Ago3 would end up with the same set of piRNAs, disrupting the piRNA amplification. We hypothesized that the regulation of Papi phosphorylation is to keep Papi free from RNA until it associates with PIWI. However, this seems to be unlikely, given that Siwi depletion had a minimal effect on Papi phosphorylation (Fig. 1g).

Zuc depletion severely decreased the levels of Siwi- and Ago3-loaded piRNAs (Fig. 2a and Extended Data Fig. 6a). In sharp contrast, RT3-1 piRNA intermediates strongly accumulated in the Papi complex after Zuc depletion (Fig. 2b and Extended Data Fig. 5c). The depletion of Trim did not lead to the accumulation of int-piRNAs (Fig. 2c and Extended Data Fig. 6b). The levels of Trim and *Nbr* (examined by western blotting and quantitative PCR, respectively) were unaffected by Zuc loss (Extended Data Fig. 6b, c). Thus, Zuc is responsible for piRNA processing in BmN4 cells.

Papi, Zuc and Trim are present in the BmN4 mitochondrial fraction (Fig. 2d). In sucrose density-gradient experiments, Zuc and Papi were detected more strongly in lower-density fractions (Fig. 2e, fractions 3–8), whereas Trim was mostly found in higher-density ones (Fig. 2e, fractions 10–12). Zuc co-immunoprecipitated with Papi and Siwi (Fig. 2f). The mitochondrial Siwi complex contained Papi and Zuc (Extended Data Fig. 6d). The interaction of Zuc with the Papi–Siwi complex during the 3′-end piRNA processing was suggested.

We sequenced the libraries generated from 65–100-nucleotide-long RNAs extracted from the mitochondrial Papi complex before and after Zuc depletion (Extended Data Fig. 6e). More than 98% (98.09% in control and 98.65% in Zuc knockdown) of the reads contained one or more sequences of Siwi- or Ago3-bound piRNAs, indicating that the sequenced reads correspond to intermediate piRNAs. 1U/10A biases were detected in the intermediate piRNA reads (Fig. 3a), suggesting that piRNAs are generated from the 5′ end of the int-piRNA sequences. More than half of the intermediate piRNAs had piRNAs aligned to their 5′ end (51.94% for control and 59.58% for Zuc knockdown), suggesting that a large proportion of int-piRNAs produce piRNAs from their 5′ end. Apparent phasing pattern was not detected within piRNAs mapped to the same intermediate (Extended Data Fig. 6f), agreeing with the previous report demonstrating that exogenous piRNAs in BmN4 cells showed only weak phasing[25]. In *Drosophila*, phased piRNAs are loaded onto Piwi and transcriptionally control transposons. However, *Bombyx* lacks a Piwi homologue and relies solely on cytoplasmic PIWIs to silence transposons post-transcriptionally. Therefore, our finding that *Bombyx* produces no phased piRNAs appears reasonable.

We examined the distance from the 3′ end of each int-piRNA to the 5′ end of the next downstream intermediate, and found that the most common 3′-to-5′ distance was 1 nucleotide (Fig. 3b). This suggests that a single cleavage event, possibly by the Siwi or Ago3 slicer, produces the 3′ end of one int-piRNA and the 5′ end of the adjacent downstream int-piRNA, as in the case of the phased piRNAs. We then focused on the cleavage site of two adjacent int-piRNAs and analysed the population of piRNAs that possess 10-nucleotide complementarity at the cleavage site (Fig. 3c). More than 94% (94.21% for control and 98.31% for Zuc knockdown) of adjacent int-piRNA pairs had piRNAs that were complementary to 10 nucleotide from the 5′ end of the downstream int-piRNA and the 3′ end of the upstream int-piRNA. In addition, we calculated the proportion of int-piRNAs with complementary piRNA at each position from the 5′ end of the downstream int-piRNA, which was found to be highest at the 10-nt position for both Siwi- and Ago3-associated piRNAs (Fig. 3d). These results suggest that Siwi and Ago3 generate both 5′ and 3′ ends of int-piRNAs by slicer activity. This was observed in both control and Zuc-depleted BmN4 cells (Fig. 3), suggesting that Zuc is not involved in the production of both 5′ and 3′ ends of int-piRNAs.

Alteration of His169 at the active site of *Drosophila* Zuc to alanine abolished its endonuclease activity[18]. Incubation of recombinant wild-type *Bombyx* Zuc, but not the corresponding mutant His141Ala, with a naked 50-nucleotide RNA (1U50) produced 7–31-nucleotide RNAs dose-dependently (Fig. 4a and Extended Data Fig. 7a–c). Zuc may preferentially cleave after cytosine, and given that the 3′ side of guanine tends to be avoided, A–C/A and U–C/U/G may rarely be cleaved (Extended Data Fig. 7c). The cleavage pattern of an 80-nucleotide RNA, a 30-nucleotide extended version of 1U50 at the 3′ end, was very similar to that of 1U50 (Extended Data Fig. 7d, e). The predicted structures of the two RNA molecules were different (data not shown), suggesting that high-dimensional structures have a low effect on Zuc cleavage.

When RNA substrate was pre-loaded onto Flag-tagged Siwi, the product size was mostly in the range of 27–31 nucleotides (Fig. 4b and Extended Data Fig. 7f, g), which are typical or permissible sizes

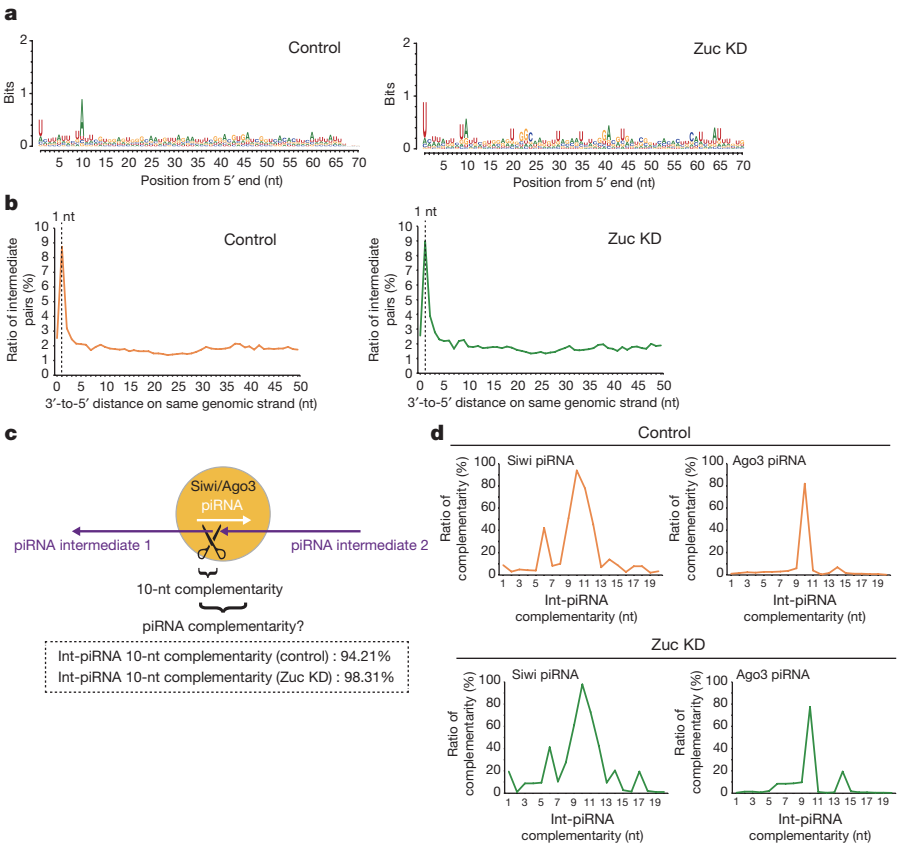

Figure 3 | Papi-associated int-piRNAs are generated by Siwi and Ago3 slicer. a, Nucleotide bias of 65–100-nucleotide Papi-associated int-piRNAs in control and Zuc-depleted cells. **b**, Analyses of distance between Papi-associated intermediates in control and Zuc-depleted BmN4 cells. The distance between the 3′ end of the upstream intermediate and the 5′ end of the downstream intermediate on the same genomic strand is analysed. **c**, Illustration showing the cleavage of adjacent intermediates by Siwi or Ago3. The frequencies of the presence of a complementary piRNA within 10 nucleotides from the 5′ end of the downstream intermediate (piRNA intermediate 1) and 3′ end of the upstream intermediate (piRNA intermediate 2) are indicated for control and Zuc-knockdown cells. **d**, Complementarity between piRNAs and adjacent intermediate sequence pairs. Graphs indicate the relative frequencies of the presence of a complementary piRNA (*y* axis), with the indicated distance at the downstream intermediate (*x* axis).

for silkworm piRNAs[14]. Similar results were obtained when the Siwi–RNA complex was pre-incubated with Papi (Fig. 4c and Extended Data Fig. 7h). Wild-type Zuc also processed RT3-1 int-piRNAs within the endogenous Papi complex to mature RT3-1 piRNA (Fig. 4d). Thus, Zuc endonuclease is the piRNA 3′-end processing factor in silkworm germline cells.

A new model for piRNA biogenesis in silkworm germline cells is shown in Extended Data Fig. 8a. In *Bombyx*, Papi might bind int-piRNAs towards the 3′ end, whereas the int-piRNA 5′ end is held by Siwi, most likely inserted into the 5′ binding pocket[26] (Extended Data Fig. 8a, b). Under this structural arrangement, it would be nearly impossible for Trim or Nbr to process int-piRNAs from the very 3′ end to mature piRNAs because Papi acts as an obstacle to the 3′-to-5′ exonuclease reaction. Zuc is an endonuclease and so is able to process int-piRNAs even under such circumstances. Zuc shows only a subtle nucleotide preference in RNA cleavage. This unique trait helps the protein to act like an 'exonuclease', as a replacement of Nbr in *Drosophila*, to determine the length of piRNA in the biogenesis pathway.

In mouse testes, the loss of the Papi homologue TDRKH (also known as TDRD2) causes piRNA precursors to be accumulated on PIWI, because without Papi, nucleases responsible for piRNA 3′-end formation, such as Zuc (known as MITOPLD in mice) and/or Trim, are incapable of processing the 3′ end[17,19,27,28]. In flies, the loss of Papi affected piRNA phasing, but hardly affected the levels of transposons in germ cells[6,29]. The piRNA pathway is highly conserved among animal species, but species diversity is evident from a mechanistic perspective.

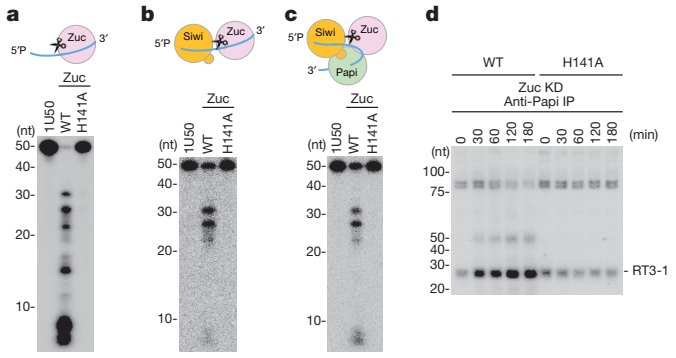

Figure 4 | Zuc processes int-piRNAs to mature piRNAs. a, Recombinant wild-type Zuc, but not the catalytically inactive Zuc(H141A) mutant, cleaves a naked 50-nucleotide RNA (1U50) *in vitro*. **b**, Wild-type Zuc cleaves 1U50 loaded onto Siwi. **c**, Wild-type Zuc cleaves 1U50 loaded onto the Papi–Siwi complex. **d**, Wild-type Zuc processes RT3-1 int-piRNAs accumulated in the Papi complex by Zuc depletion to mature RT3-1 piRNAs.

Online Content Methods, along with any additional Extended Data display items and Source Data, are available in the online version of the paper; references unique to these sections appear only in the online paper.

Received 12 June 2017; accepted 26 January 2018.
Published online 28 February 2018.

1. Ghildiyal, M. & Zamore, P. D. Small silencing RNAs: an expanding universe. *Nat. Rev. Genet.* **10,** 94–108 (2009).

2. Iwasaki, Y. W., Siomi, M. C. & Siomi, H. PIWI-interacting RNA: its biogenesis and functions. *Annu. Rev. Biochem.* **84,** 405–433 (2015).
3. Czech, B. & Hannon, G. J. One loop to rule them all: the ping-pong cycle and piRNA-guided silencing. *Trends Biochem. Sci.* **41,** 324–337 (2016).
4. Izumi, N. *et al.* Identification and functional analysis of the pre-piRNA 3′ Trimmer in silkworms. *Cell* **164,** 962–973 (2016).
5. Honda, S. *et al.* Mitochondrial protein BmPAPI modulates the length of mature piRNAs. *RNA* **19,** 1405–1418 (2013).
6. Han, B. W., Wang, W., Li, C., Weng, Z. & Zamore, P. D. Noncoding RNA. piRNA-guided transposon cleavage initiates Zucchini-dependent, phased piRNA production. *Science* **348,** 817–821 (2015).
7. Mohn, F., Handler, D. & Brennecke, J. Noncoding RNA. piRNA-guided slicing specifies transcripts for Zucchini-dependent, phased piRNA biogenesis. *Science* **348,** 812–817 (2015).
8. Hayashi, R. *et al.* Genetic and mechanistic diversity of piRNA 3′-end formation. *Nature* **539,** 588–592 (2016).
9. Brennecke, J. *et al.* Discrete small RNA-generating loci as master regulators of transposon activity in *Drosophila*. *Cell* **128,** 1089–1103 (2007).
10. Gunawardane, L. S. *et al.* A slicer-mediated mechanism for repeat-associated siRNA 5′ end formation in *Drosophila*. *Science* **315,** 1587–1590 (2007).
11. Homolka, D. *et al.* PIWI slicing and RNA elements in precursors instruct directional primary piRNA biogenesis. *Cell Reports* **12,** 418–428 (2015).
12. Saito, K. *et al.* A regulatory circuit for *piwi* by the large Maf gene *traffic jam* in *Drosophila*. *Nature* **461,** 1296–1299 (2009).
13. Kawaoka, S. *et al.* The *Bombyx* ovary-derived cell line endogenously expresses PIWI/PIWI-interacting RNA complexes. *RNA* **15,** 1258–1264 (2009).
14. Nishida, K. M. *et al.* Respective functions of two distinct Siwi complexes assembled during PIWI-interacting RNA biogenesis in *Bombyx* germ cells. *Cell Reports* **10,** 193–203 (2015).
15. Xiol, J. *et al.* A role for Fkbp6 and the chaperone machinery in piRNA amplification and transposon silencing. *Mol. Cell* **47,** 970–979 (2012).
16. Liu, L., Qi, H., Wang, J. & Lin, H. PAPI, a novel TUDOR-domain protein, complexes with AGO3, ME31B and TRAL in the nuage to silence transposition. *Development* **138,** 1863–1873 (2011).
17. Ipsaro, J. J., Haase, A. D., Knott, S. R., Joshua-Tor, L. & Hannon, G. J. The structural biochemistry of Zucchini implicates it as a nuclease in piRNA biogenesis. *Nature* **491,** 279–283 (2012).
18. Nishimasu, H. *et al.* Structure and function of Zucchini endoribonuclease in piRNA biogenesis. *Nature* **491,** 284–287 (2012).
19. Watanabe, T. *et al.* MITOPLD is a mitochondrial protein essential for nuage formation and piRNA biogenesis in the mouse germline. *Dev. Cell* **20,** 364–375 (2011).
20. Feltzin, V. L. *et al.* The exonuclease Nibbler regulates age-associated traits and modulates piRNA length in *Drosophila*. *Aging Cell* **14,** 443–452 (2015).
21. Horwich, M. D. *et al.* The *Drosophila* RNA methyltransferase, DmHen1, modifies germline piRNAs and single-stranded siRNAs in RISC. *Curr. Biol.* **17,** 1265–1272 (2007).
22. Saito, K. *et al.* Pimet, the *Drosophila* homolog of HEN1, mediates 2′-*O*-methylation of Piwi- interacting RNAs at their 3′ ends. *Genes Dev.* **21,** 1603–1608 (2007).
23. Eddy, E. M. Germ plasm and the differentiation of the germ cell line. *Int. Rev. Cytol.* **43,** 229–280 (1975).
24. Nicastro, G., Taylor, I. A. & Ramos, A. KH-RNA interactions: back in the groove. *Curr. Opin. Struct. Biol.* **30,** 63–70 (2015).
25. Shoji, K., Suzuki, Y., Sugano, S., Shimada, T. & Katsuma, S. Artificial "ping-pong" cascade of PIWI-interacting RNA in silkworm cells. *RNA* **23,** 86–97 (2017).
26. Matsumoto, N. *et al.* Crystal structure of silkworm PIWI-clade Argonaute Siwi bound to piRNA. *Cell* **167,** 484–497.e9 (2016).
27. Saxe, J. P., Chen, M., Zhao, H. & Lin, H. Tdrkh is essential for spermatogenesis and participates in primary piRNA biogenesis in the germline. *EMBO J.* **32,** 1869–1885 (2013).
28. Ding, D. *et al.* PNLDC1 is essential for piRNA 3′ end trimming and transposon silencing during spermatogenesis in mice. *Nat. Commun.* **8,** 819 (2017).
29. Handler, D. *et al.* A systematic analysis of *Drosophila* TUDOR domain-containing proteins identifies Vreteno and the Tdrd12 family as essential primary piRNA pathway factors. *EMBO J.* **30,** 3977–3993 (2011).

Supplementary Information is available in the online version of the paper.

Acknowledgements We are grateful to T. Mannen for preparing materials for mass spectrometry, T. Suzuki for comments on our *in vitro* Zuc processing assays and Y. Ono for support with the bioinformatics. We also thank S. Ohnishi for technical assistance and other members of the Siomi laboratories for discussions and comments on the manuscript. This work was supported by grants from the Ministry of Education, Culture, Sports, Science and Technology of Japan to K.M.N., Y.W.I., Y.M., H.S. and M.C.S. R.M. is supported by CREST, the Japan Science and Technology Agency. T.Ka. was supported by grants from the New Energy and Industrial Technology Development Organization, Japan, and Translational Systems Biology and Medicine Initiative from the Ministry of Education, Culture, Sports, Science and Technology of Japan. T.Ko. is a recipient of Molecular Dynamics for Antibody Drug Development, First Program Grant from the Japan Society of Promotion of Science.

Author Contributions K.M.N. generated monoclonal antibodies and performed biochemical analyses of piRNAs, int-piRNAs and piRNA factors. K.S. carried out *in vitro* experiments with help from R.M. H.Y. performed protein–protein interaction analyses. Y.M. performed immunofluorescence analyses. Y.W.I. performed bioinformatics analyses. T.Ka. and T.Ko. performed LC–MS/MS analysis. M.C.S. designed the experiments with other authors, supervised and discussed the work, and wrote the manuscript. H.S. discussed and supervised the study. All authors commented on the manuscript.

Author Information Reprints and permissions information is available at www.nature.com/reprints. The authors declare no competing financial interests. Readers are welcome to comment on the online version of the paper. Publisher's note: Springer Nature remains neutral with regard to jurisdictional claims in published maps and institutional affiliations. Correspondence and requests for materials should be addressed to M.C.S. (siomim@bs.s.u-tokyo.ac.jp).

Reviewer Information *Nature* thanks J. Brennecke, S. Chameyron and the other anonymous reviewer(s) for their contribution to the peer review of this work.

METHODS

Production of monoclonal antibodies. Monoclonal antibodies were produced essentially as described previously[14]. Mice were immunized with bacterially produced glutathione *S*-transferase (GST)-tagged Papi (amino acids 430–629), GST–Trim (amino acids 1–240) or GST–Zuc (amino acids 63–206). The *Papi*, *Trim* and *Zuc* cDNAs corresponding to the particular regions were obtained by RT–PCR using total RNAs from BmN4 cells. The PCR primers used are summarized in the 'Oligonucleotides' section.

Plasmid construction. pIB-myc and pIB-3xFlag were generated using a pIB vector (Thermo Fisher Scientific). Vectors to express Myc–Siwi and Papi–Flag were generated by inserting *Siwi* and *Zuc* cDNAs into pIB-myc and pIB-3xFlag, respectively. Vectors for expressing the Papi–Flag KH mutant, the Papi–Flag siRNA-resistant mutant, the Flag–Siwi RK mutant and the Flag–Ago3 RK mutant were generated by inverse PCR using expression vectors for Papi–Flag (this study), Flag–Siwi[14] and Flag–Ago3[14] as templates. The PCR primers used are summarized in the 'Oligonucleotides' section.

RNAi and transgene expression. Double-stranded RNAs (dsRNAs) were produced by *in vitro* T7 transcription, followed by annealing in water. The PCR primers to generate dsRNAs are summarized in the 'Oligonucleotides' section. BmN4 cells were transfected with 2 μg of dsRNAs (per 3×10^5 cells) using FuGENE HD (Promega). To express proteins exogenously in BmN4 cells, the cells were transfected with 2 μg of plasmids (per 6×10^5 cells) using FuGENE HD.

Western blot analysis. Western blotting was carried out as described previously[14]. The Y12 antibody was a gift from G. Dreyfuss. Anti-HSP60 (StressMarq Biosciences), anti-tubulin (Developmental Studies Hybridoma Bank), anti-DDDDK-tag (Flag) (MBL), and anti-Myc (Sigma) antibodies were purchased.

qRT–PCR. qRT–PCR was performed as described previously[30]. The PCR primers used are summarized in the 'Oligonucleotides' section.

Immunoprecipitation and RNA isolation. Immunoprecipitation of Flag–Siwi and Flag–Ago3 was carried out essentially as described previously[14]. BmN4 whole and mitochondrial lysates (Fig. 2c, f and Extended Data Fig. 6d) were prepared in binding buffer (30 mM HEPES (pH 7.4), 150 mM potassium acetate, 5 mM magnesium acetate, 5 mM DTT, 0.5% Triton X-100, 2 μg ml^{-1} pepstatin, 2 μg ml^{-1} leupeptin and 0.5% aprotinin) and incubated with anti-Papi, anti-Siwi or anti-Flag antibody bound to Dynabeads (Invitrogen) at 4 °C for 2 h. The beads were washed four times with binding buffer. BmN4 whole (Fig. 1h and Extended Data Fig. 5b) and mitochondrial (Extended Data Fig. 5c) lysates were prepared in binding buffer containing 500 mM sodium chloride and incubated with anti-Papi or anti-Siwi antibody. The beads were washed twice with binding buffer containing 500 mM sodium chloride, and then twice with binding buffer. RNAs were eluted from the beads by phenol–chloroform after protease K treatment and precipitated with ethanol. RNA ^{32}P-labelling[14], β-elimination[22] and northern blotting[12] were carried out as described previously. RNAs were crosslinked to Hybond-N$^+$ (GE Healthcare) by UV irradiation. The sequences of the RT3-1 probe and siRNA used in the β-elimination experiment are described in 'Oligonucleotides'.

Generation of PIWI-associated small RNA libraries. Immunoprecipitation of Flag–Siwi and Flag–Ago3 was carried out as described previously[14]. RNAs were eluted from the immunoprecipitates by phenol–chloroform after protease K treatment, and precipitated with ethanol. RNAs of 23–35 nucleotides in length were eluted from the gels and used to generate small RNA libraries[14].

Analysis of PIWI-associated small RNA sequences. Libraries were sequenced using Illumina MiSeq (single-end, 51 cycles). For Siwi-associated small RNAs, a total of 4,547,701 reads were obtained from the control sample, 3,054,386 reads from the Trim-knockdown sample and 4,083,584 reads from the Nbr-knockdown sample. For Ago3-associated small RNAs, a total of 3,855,720 reads were obtained from the control sample, 3,702,496 reads from the Trim-knockdown sample and 3,292,910 reads from the Nbr-knockdown sample. The analysis of small RNAs was performed as described previously[14]. In brief, adaptor sequences were removed from the obtained reads, and the reads in the range of 23–35 nucleotides were used for further analysis (89–94% of the sequenced reads were in this size range). The reads were mapped to the silkworm reference genome (downloaded from the Silkworm Genome Research Program Database; http://sgp.dna.affrc.go.jp/data/integretedseq.txt.gz) using Bowtie[31], allowing no mismatches. Genome mapped reads were extracted and aligned to 121 *B. mori* transposon consensus sequences (a gift from S. Kawaoka) using Bowtie[31], allowing up to two mismatches. Using transposon-mapped reads, the length distribution was calculated. Sequence logos were calculated using the motifStack R package. The sequences were aligned to the 5′ end upon the calculation of sequence logos. Strand bias and frequency (reads per million) of small RNA reads were calculated for 70 transposon consensus sequences with higher amount of mapped Siwi and Ago3 piRNAs (reads per million) in control sample, and heat maps were depicted using Java TreeView software[32].

Dephosphorylation treatment. Immunopurified Papi was incubated with Antarctic Phosphatase (NEB) at 37 °C for 30 min for dephosphorylation.

Immunofluorescence. Immunofluorescence was carried out essentially as described previously[14]. Anti-Flag antibody and Alexa Fluor 488 goat anti-mouse IgG antibody (Invitrogen) were used as primary and secondary antibodies, respectively.

Trypsin digestion and LC–MS/MS analysis. The method for trypsin digestion of protein has been described previously[33]. Liquid chromatography–tandem mass spectrometry (LC–MS/MS) analysis was performed using an LTQ Orbitrap XL electron transfer dissociation (ETD) mass spectrometer (Thermo Fisher Scientific). The methods used for LC–MS/MS were slightly modified from those described previously[34]. The mass spectrometer was operated in a data-dependent acquisition mode in which the mass spectrometry acquisition with a mass range of m/z 420–1,600 was automatically switched to MS/MS acquisition under the automated control of Xcalibur software. The top four precursor ions in an MS scan were selected by Orbitrap, with resolution $R = 60{,}000$ and in subsequent MS/MS scans by ion trap in the automated gain control (AGC) mode in which the AGC values were 5.00×10^5 and 1.00×10^4 for full MS and MS/MS, respectively. To analyse dimethylation sites, ETD was used.

Database searching and protein identification. Database searches were performed using the MASCOT 2.5.1 search engine (Matrix Science) against the UniProtKB_2016-8 database (selected for *B. mori*), assuming trypsin as the digestion enzyme and allowing for trypsin specificity of up to four missed cleavages. The database was searched with a fragment ion mass tolerance of 0.60 Da and a parent ion tolerance of 3.0 p.p.m. The iodoacetamide derivative of cysteine was specified as a fixed modification and methylation of arginine, oxidation of methionine, dimethylation of arginine and acetylation of N termini were specified as variable modifications. Scaffold (version Scaffold_4.7.5; Proteome Software) was used to validate MS/MS-based peptide and protein identifications. We accepted the peptide identifications when the Peptide Prophet algorithm[35] specified probabilities at >95.0%. Sequence coverage was defined as the percentage of the protein in the identified peptide sequence.

CLIP. CLIP was performed as described previously[36]. Dephosphorylation and RNA radiolabelling with ^{32}P were performed using T4 polynucleotide kinase.

Rescue assay. BmN4 cells were transfected with 500 pmol siRNA duplex (per 1×10^6 cells) using Cell Line Nucleofector Kit L (Lonza) and incubated at 27 °C for 72 h. The sequences of siRNAs are presented in 'Oligonucleotides'. After RNAi, cells were transfected with 2 μg of Papi–Flag plasmid using FuGENE HD and incubated at 27 °C for 72 h. Cells were then transfected with 2 μg Myc–Siwi plasmid and incubated at 27 °C for 24 h. BmN4 lysates were prepared in binding buffer (30 mM HEPES (pH 7.4), 150 mM potassium acetate, 5 mM magnesium acetate, 5 mM dithiothreitol (DTT), 0.1% Tergitol-type NP-40, 2 μg ml^{-1} pepstatin, 2 μg ml^{-1} leupeptin and 0.5% aprotinin) containing 500 mM sodium chloride, and incubated with anti-Myc antibody bound to Dynabeads. The beads were washed twice with binding buffer containing 500 mM sodium chloride and then twice with binding buffer. RNAs were eluted from the beads by phenol-chloroform after protease K treatment and precipitated with ethanol. RNA radiolabelling was carried out as described previously[14].

Sucrose density gradient centrifugation. Mitochondria were prepared as described previously[37]. The mitochondrial pellet was resuspended in gradient buffer (30 mM HEPES (pH 7.4), 100 mM potassium acetate, 1 mM DTT, 4 mM magnesium acetate, and 1% Tergitol-type NP-40), and centrifuged at 14,000*g* at 4 °C for 30 min. The supernatant was placed at the top of a 10–40% sucrose gradient and centrifuged in a Beckman MLS-50 rotor at 178,000*g* at 4 °C for 16.5 h.

Preparation of Papi-associated int-piRNA libraries. RNAs were eluted from the Papi immunoprecipitates by phenol–chloroform after protease K treatment and precipitated with ethanol. RNAs were resolved by denaturing PAGE, and 65–100-nucleotide-long RNAs were eluted from gels. The libraries were generated as described previously[14].

Sequence analysis of Papi-associated int-piRNAs. Libraries were sequenced using Illumina MiSeq (single-end, 111 cycles). A total of 10,584,873 reads were obtained from the control sample and 7,932,439 reads were obtained from the Zuc-knockdown sample. Adaptor sequences were removed from the obtained reads, and the reads were mapped to the silkworm reference genome (downloaded from the Silkworm Genome Research Program Database; http://sgp.dna.affrc.go.jp/data/integretedseq.txt.gz) using Bowtie[31], allowing no mismatches. Genome mapped reads were extracted and aligned to *B. mori* transposon consensus sequences using Bowtie[31], allowing up to two mismatches. To reduce the effect of contaminant reads, the reads mapped to transposon consensus sequences were used for further analysis. Sequence logos were calculated using the motifStack R package (http://www.bioconductor.org/packages/release/bioc/html/motifStack.html). The sequences were aligned to the 5′ end upon the calculation of sequence logos. Calculations of the distance between intermediates and piRNA-phasing analysis were performed as previously described[6], and complementarity of piRNAs and adjacent intermediate pairs was calculated using an in-house script.

The phasing analysis and piRNA-intermediate complementarity calculation were performed using each pair of intermediates preserving the read count. Siwi and Ago3 piRNA sequences were obtained from previously published data[14] (GEO accession GSE58221).

Recombinant protein preparation. The cDNA encoding Zuc excluding MLS (residues 29–206) was cloned into pCold-GST vector. The Zuc(H141A) mutant was generated from pCold-Zuc by inverse PCR. The protein was purified using glutathione-Sepharose (GE Healthcare) with purification buffer (20 mM Tris-HCl (pH 8.0), 150 mM sodium chloride and 1 mM DTT). The proteins were treated with HRV3C protease (GE Healthcare) to remove the GST tag and further purified by Enrich S (Bio-Rad). To yield pIZ-3xFlag-Siwi, 3xFlag-Siwi was amplified from pIB-3xFlag-Siwi[14] by PCR and inserted into pIZ vector (Thermo Fisher). Flag–Siwi was immunoisolated by ANTI-FLAG M2 Affinity Gel (Sigma) from BmN4 cells and eluted by 500 ng μl^{-1} 3× Flag peptide (Sigma).

***In vitro* processing assay.** The synthesized RNAs (GeneDesign) were ^{32}P-labelled at their 5′ end. The sequences of RNAs are indicated in 'Oligonucleotides;. Radiolabelled int-piRNAs (10^4 c.p.m.) were incubated with 0.1 μg of recombinant Zuc in 20 μl of buffer A[18] at 26 °C for 30 min. A total of 1 μl of 1 μM radiolabelled int-piRNAs and 200 ng of purified Flag–Siwi were mixed at 26 °C for 30 min in 20 μl of the loading buffer (30 mM HEPES (pH 7.4), 100 mM potassium acetate, 2 mM magnesium acetate, 20 mM creatine monophosphate, 1 mM ATP, 0.15 U μl^{-1} creatine phosphokinase, 1 mM DTT and 0.5 U μl^{-1} RNasin (Promega)). After loading, the Flag–Siwi-containing mixture was incubated with Dynabeads (with anti-Siwi antibody or Papi immunoprecipitation product) at 4 °C for 1 h. The beads were then washed five times with binding buffer. RNAs were isolated from the beads with phenol–chloroform and precipitated with ethanol. They were then resolved by denaturing PAGE. Immunopurified Papi complexes were incubated with 1 μg of recombinant Zuc in 30 μl of buffer A[18] containing 2.5 mM EGTA and 0.1 U μl^{-1} RNasin at 27 °C for 0–180 min. RNAs were isolated from the beads with phenol–chloroform and precipitated with ethanol, after which they were transferred to Hybond-N (GE Healthcare). Next, RNAs were chemically crosslinked to membrane using 1-ethyl-3-(3-dimethylaminopropyl) carbodiimide as described previously[14]. The sequence of probe RT3-1 is indicated in the 'Oligonucleotides' section.

Oligonucleotides. Primers used for producing constructs for Myc–Siwi, Papi–Flag, siRNA-resistant Papi, Papi KH mutant, Flag–Siwi RK mutant, Flag–Ago3 RK mutant and pIZ-3xFlag-Siwi are listed below.

Myc-L (left, forward): 5′-TTCGAATTTAAAGCTCACCATGGGA GAGCAGAAACTGATC-3′, Myc-R (right, reverse): 5′-CTGCAGGAATTCGAT CCGGGTACCAAGCTTGCTAG-3′; 3xFlag-L: 5′-GGCCCGCGGTTCGAAGA CTACAAAGACCAT-3′, 3xFlag-R: 5′-AGTCAGATAAACTCAGATATCCT TGTCATC-3′; Myc–Siwi-L: 5′-TGCAGCCCAGCGCTGGATCCATG TCAGAACCGAGAGGTAG-3′, Myc–Siwi-R: 5′-CGAACCGCGGGCCCTTTAG AGGAAATATAAAGTTT-3′; Papi–Flag-L: 5′-TCGAATTTAAAGCTTATGT CATTGAACACAAAATT-3′, Papi–Flag-R: 5′-GAACCGCGGGCCCTCCTTT TCAAAAGCGGACTTAC-3′; Papi siRNA-res-L: 5′-CACCCAAGTCAACAGA TAAAGTTGCTGAGCA-3′, Papi siRNA-res-R: 5′-ACTCCACTTTGACGCGA GCGCCACTGCGAT-3′; Papi KH I69N mut-L: 5′-TCCAACAACAAGGACC TTCAGAAGAAATCT-3′, Papi KH I69N mut-R: 5′-GCCATTGCGACCAAT CAGAGCTGGAACAAT-3′; Papi KH V142N mut-L: 5′-GAGAACAACAATGA TATTAGCCATCGCAGT-3′, Papi KH V142N mut-R: 5′-ACCTCCAGATCCAATT ATTCTCCCACAAGA-3′; Siwi RK mut1-L: 5′-CAGAACCGAGAGGTAAAG GAAAAGCTAAAGGAAAGGCTGGTAAGGGTGGTGATGGAGGC-3′, Siwi RK mut1-R: 5′-GCCTCCATCACCACCCTTACCAGCCTTTCCTTTAGCTTT TCCTTTACCTCTCGGTTCTG-3′; Siwi RK mut2-L: 5′-CGTAGTTGGCAAG GGCTCTAAAAAAGGGGGTGGAAAAGTCCTTCCTG-3′, Siwi RK mut2-R: 5′-CAGGAAGGACTTTTCCACCCCCTTTTTTAGAGCCCTTGCCAACTACG-3′; Ago3 RK mut1-L: 5′-CCAGGCAAAGGCAAGGGGAAAAGCTTAGCCC-3′, Ago3 RK mut1-R: 5′-GGGCTAAGCTTTTCCCCTTGCCTTTGCCTGG-3′; Ago3 RK mut2-L: 5′-GTATAGGCGGTAAAGGAAAGGCAGCAGCATTG-3, Ago3 RK mut2-R: 5′-CAATGCTGCTGCCTTTCCTTTACCGCCTATAC-3′; Ago3 RK mut3-L: 5′-CAGCTGGAACTGGAAAGGGATTCAAATTGC-3′Ago3 RK mut3-R: 5′-GCAATTTGAATCCCTTTCCAGTTCCAGCTG-3′; 3xFlag-Siwi-L: 5′-TCGAATTTAAAGCTTCACCATGGACTACAAAGACCATGACGGTG-3′, 3xFlag-Siwi-R: 5′-GAACGAGAAACGTAAAAGTTTAGAGGAAATATA AAGTTTCATTC-3′.

Primers used for producing constructs for GST–Papi, GST–Trim and GST–Zuc are: GST–Papi-L: 5′-TGGGATCCCCGAATTCAAGGACAAAGAGATACCTGG-3′, GST–Papi-R: 5′-GGCCGCTCGAGTCGACTCACTTTTCAAAAGCGGACT-3′; GST–Trim-L: 5′-TGGGATCCCCGAATTCATGGATATCACCAAAGAAAA-3′, GST–Trim-R: 5′-GGCCGCTCGAGTCGACTTAGTTATCTTCCAGTA TTGCTA-3′; GST–Zuc-L: 5′-TACCCTCGAGGGATCCACAAAAAGCATG GAC-3′, GST–Zuc-R: 5′-CGACAAGCTTGAATTTTAACTGGTTATTGG-3′.

Primers used for producing constructs for pCold-Zuc and the Zuc(H141A) mutant are: pCold-Zuc-L: 5′-TACCCTCGAGGGATCCAAGAAGAAGAA AGAA-3′, pCold-Zuc-R: 5′-CGACAAGCTTGAATTTTAACTGGTTATTGG-3′; Zuc(H141A)-L: 5′-GCCCACAAGTTCTGCATAATAGATG-3′, Zuc(H141A)-R: 5′-CATTAGATTTGTAGACTTCATCCAG-3′.

Primers used to generate templates for dsRNA production are: T7-dsLuc-L: 5′-TAATACGACTCACTATAGGGGGAGAGCAACTGCATAAGGC-3′, T7-dsLuc-R: 5′-TAATACGACTCACTATAGGGTCCCTATCGAA GGACTCTGG-3′; T7-dsPapi-L: 5′-TAATACGACTCACTATAGGGTC TAGTGACATTCCGTGGTA-3′, T7-dsPapi-R: 5′-TAATACGACTCACTATAGG GAGCACTCCATGGCCTGGAAC-3′; T7-dsTrim-L: 5′-TAATACGACTCAC TATAGGGTTCAGAAGTTTCAAAATGGT-3′, T7-dsTrim-R: 5′-TAATACGAC TCACTATAGGGAGCGAAGAATTCATACAAAT-3′; T7-dsZuc-L: 5′-TAATAC GACTCACTATAGGGATGGCAGTAACTCTTAGTAA-3′, T7-dsZuc-R: 5′-TAATACGACTCACTATAGGGGTCCAGTTCAATGACCCTGC-3′; T7-dsNbr-L: 5′-TAATACGACTCACTATAGGGACAAATTGTTATGGCATTGG-3′, T7-dsNbr-R: 5′-TAATACGACTCACTATAGGGCAATCCATTTCAAGGCTTCA-3′; T7-dsSiwi-L: 5′-TAATACGACTCACTATAGGGGCAAATAATGTCAAATACCC-3′, T7-dsSiwi-R: 5′-TAATACGACTCACTATAGGGACCACCATCAGTGACGGCAG-3′.

Sequences of siRNA duplexes used for RNAi (DNA: normal font, RNA: underlined) are: Luc siRNA duplex: 5′-CGUACGCGGAAUACUUCGATT-3′ and 5′-UCGAAGUAUUCCGCGUACGTT-3′; Papi siRNA duplex: 5′-GGUCG AAAGUCCUAAAAGUTT-3′ and 5′-ACUUUUAGGACUUUCGACCTT-3′.

Sequence of RT3-1 probe used for northern blot is: 5′-ACCAGCCGATCGTC ATCGCATCCGTTTA-3′. Sequence of siRNA used for β-elimination is: 5′-UGGUCU GCCUAAAGGUGUCGCUCUGC-3′. Primers used for qPCR are: Nbr-L: 5′-ACAGCCAGTTCAAAATAGTTATTGC-3′, Nbr-R: 5′-TTGACCACAGT ATTCACACAGAACT-3′; Rpl3-L: 5′-GGTGTCACCAAGGGCAAAGG-3′, Rpl3-R: 5′-AGGATGCCAAGCTCCAATGC-3′.

Sequences of RNA used for processing assays are: 1U29: 5′-UCAAA AACUAACGGAUUGGUUUCGAACAG-3′; 1U50: 5′-UCAAAAACUAACGGAU UGGUUUCGAACAGUCACCCGCCCGGACAGGUCCC-3′; 1U80: 5′-UCAA AAACUAACGGAUUGGUUUCGAACAGUCACCCGCCCGGACAGGUCCC CUACCUGUCCCUAAUCAACUGGCAGCCGGG-3′.

Statistics and reproducibility. Experiments in Figs 1a, e, 2b–e and 4d were performed three times independently with similar results. Experiments in Figs 1b–d, f–h, 2a, f and 4a–c were performed twice independently with similar results. Experiments in Extended Data Figs 1b, c, 4b, 5b, c, f, g, 6a, b were performed three times independently with similar results. Experiments in Extended Data Figs 3a, 4a, c, d, 5a, d, e, h, 6d and 7a–h were performed twice independently with similar results. Experiments in Extended Data Fig. 3c were performed once. No statistical methods were used to predetermine sample size. The experiments were not randomized, and investigators were not blinded to allocation during experiments and outcome assessment.

Data availability. Gel source images for Figs 1a–h, 2a–f and 4a–d and Extended Data Figs 1b, c, 3a, 4a, b, d, 5a–h, 6a, b, d and 7a–h are available in Supplementary Fig. 1. All other data supporting the findings of this study are available from the corresponding author upon reasonable request. All sequencing data that support the findings of this study were deposited in the NCBI Gene Expression Omnibus (GEO) with the GEO series accession number GSE107371.

30. Sumiyoshi, T. *et al.* Loss of *l(3)mbt* leads to acquisition of the ping-pong cycle in *Drosophila* ovarian somatic cells. *Genes Dev.* **30,** 1617–1622 (2016).
31. Langmead, B., Trapnell, C., Pop, M. & Salzberg, S. L. Ultrafast and memory-efficient alignment of short DNA sequences to the human genome. *Genome Biol.* **10,** R25 (2009).
32. Saldanha, A. J. Java Treeviewextensible visualization of microarray data. *Bioinformatics* **20,** 3246–3248 (2004).
33. Fujinoki, M. *et al.* Identification of 36-kDa flagellar phosphoproteins associated with hamster sperm motility. *J. Biochem.* **133,** 361–369 (2003).
34. Fujii, K. *et al.* Fully automated online multi-dimensional protein profiling system for complex mixtures. *J. Chromatogr. A* **1057,** 107–113 (2004).
35. Keller, B. O., Wang, Z. & Li, L. Low-mass proteome analysis based on liquid chromatography fractionation, nanoliter protein concentration/digestion, and microspot matrix-assisted laser desorption ionization mass spectrometry. *J. Chromatogr. B Analyt. Technol. Biomed. Life Sci.* **782,** 317–329 (2002).
36. Murota, Y. *et al.* Yb integrates piRNA intermediates and processing factors into perinuclear bodies to enhance piRISC assembly. *Cell Rep.* **8,** 103–113 (2014).
37. Wieckowski, M.R., Giorgi, C., Lebiedzinska, M., Duszynski, J., & Pinton, P. Isolation of mitochondria-associated membranes and mitochondria from animal tissues and cells. *Nat. Protocols* **4,** 1582–1590 (2009).

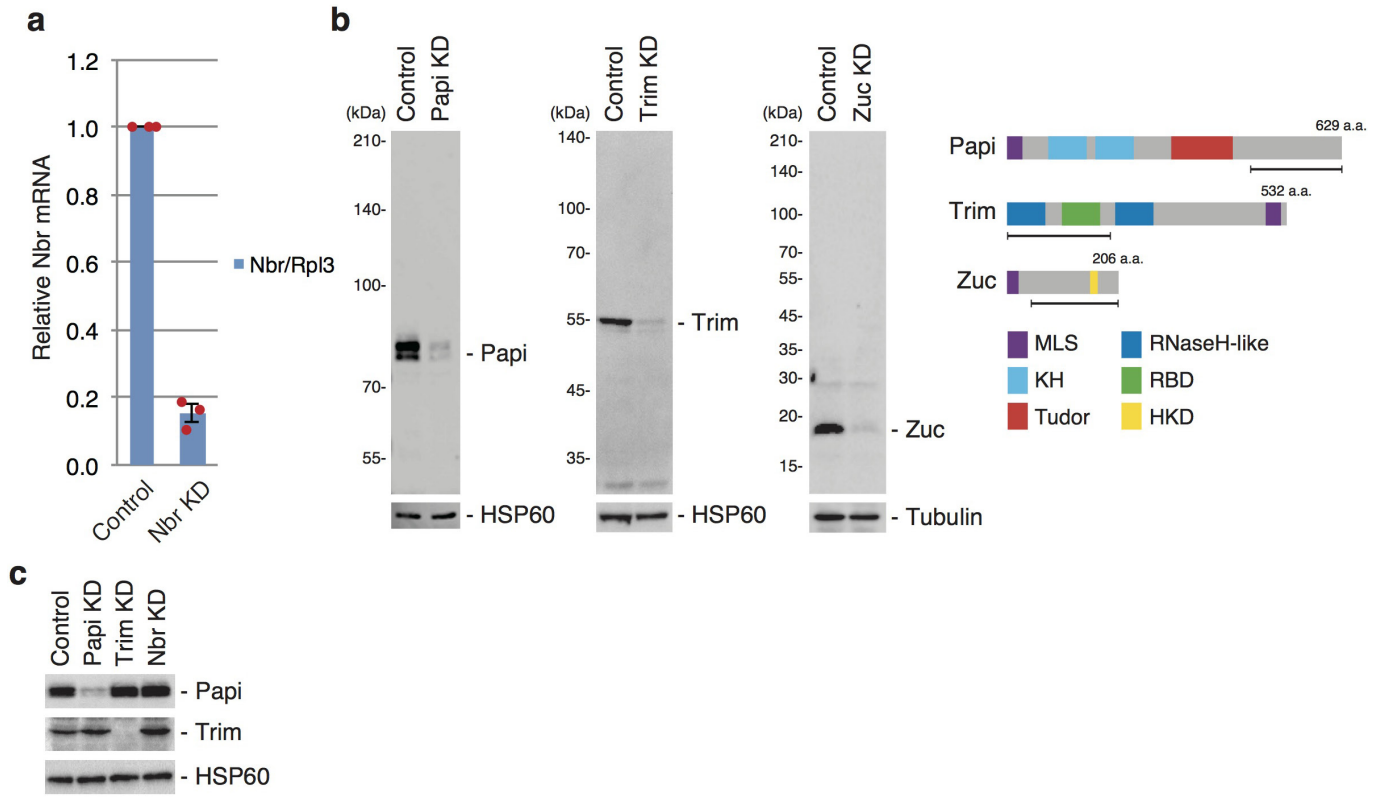

Extended Data Figure 1 | Production of monoclonal antibodies against Papi, Trim and Zuc, and analysis of depletion upon RNA interference treatment. a, Quantitative PCR with reverse transcription (qRT–PCR) shows that *Nbr* was efficiently depleted by RNA interference (RNAi) in BmN4 cells. Data are mean ± s.e.m. of three independent experiments. **b**, Western blotting shows the specificity of anti-Papi, anti-Trim and anti-Zuc monoclonal antibodies raised in this study. HSP60 and tubulin were used as loading controls. The images show the domain structures of Papi, Trim and Zuc. Underlines indicate the antigen regions used for producing the monoclonal antibodies. **c**, Western blotting shows that Papi and Trim were efficiently depleted by RNAi in BmN4 cells.

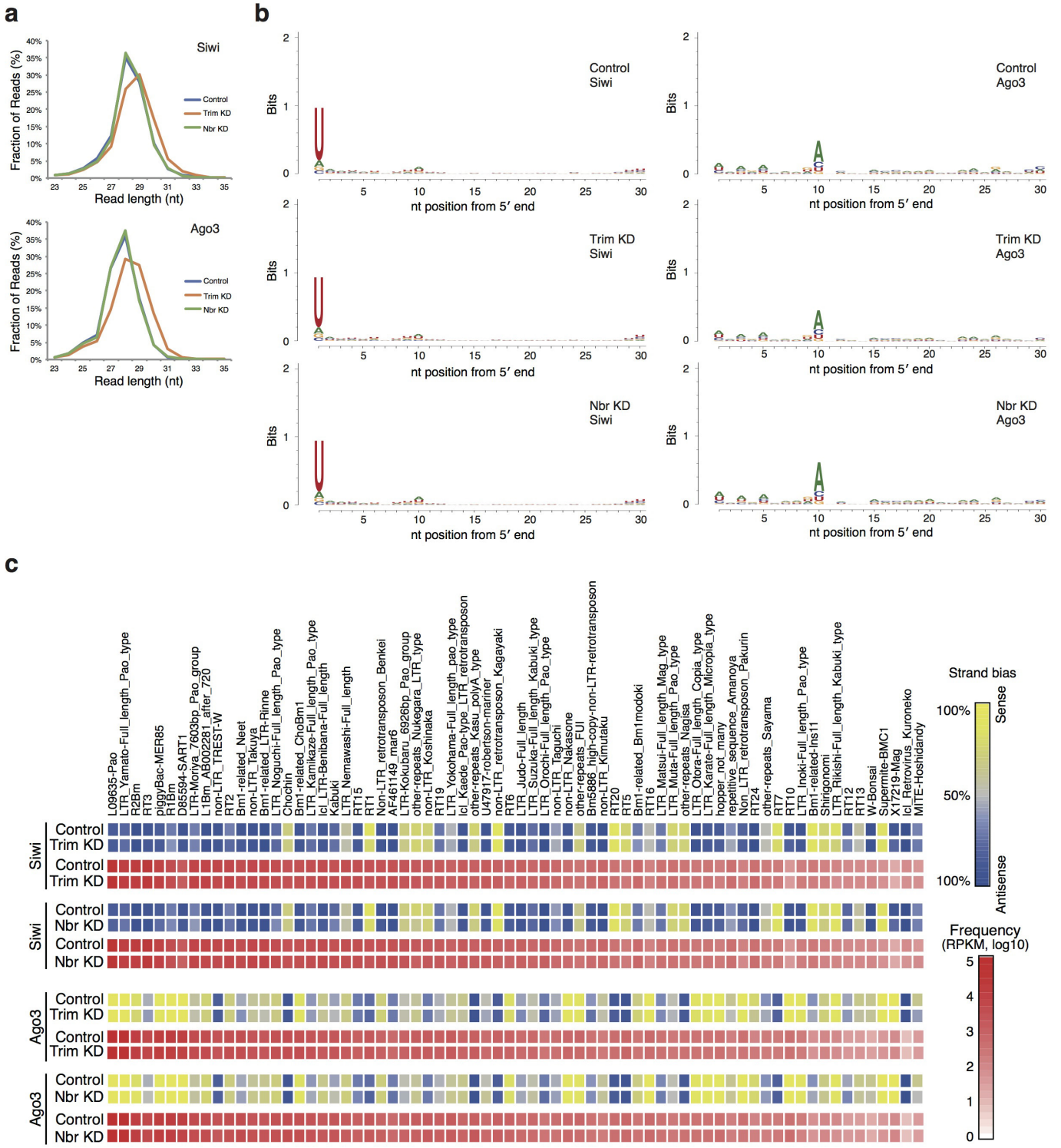

Extended Data Figure 2 | Siwi/Ago3-associated small RNAs upon Trim or Nbr depletion. a, Length distribution of transposon-mapped Flag-Siwi- and Flag-Ago3-associated piRNAs. piRNAs appear to be slightly longer when Trim was depleted. **b**, Sequence logos showing unaffected levels of 1U and 10A under Trim- or Nbr-depleted conditions. **c**, Strand bias and frequency of piRNAs mapped to each transposon consensus sequence. Depletion of Trim or Nbr has little effect on strand bias or the frequency of piRNAs mapped to each transposon consensus sequence.

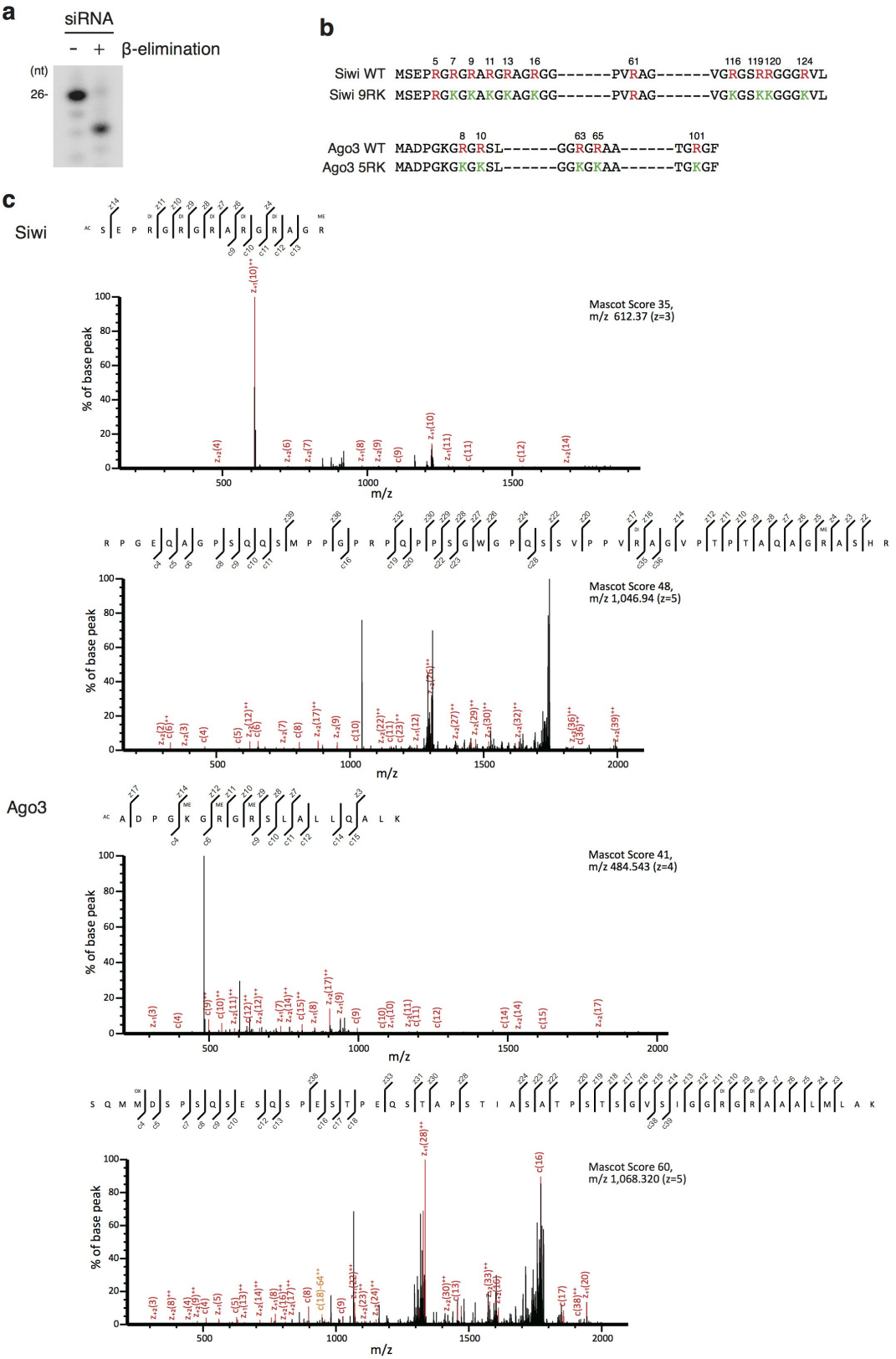

Extended Data Figure 3 | sDMA modification of Siwi and Ago3. **a**, A synthesized short interfering RNA (siRNA) (26 nucleotides) was downshifted by β-elimination, indicating that this siRNA is not 2′-*O*-methylated. **b**, The amino acid sequences of the N-terminal regions of wild-type Siwi, the Siwi-9RK mutant, wild-type Ago3 and the Ago3-5RK mutant are shown. Arginine residues shown in red were determined to be sDMAs in BmN4 cells. Arginine residues mutated to lysines are shown in green. **c**, Representative ETD tandem mass spectra for Siwi and Ago3 peptides, which include arginine modifications. Ac, acetylation; Di, demethylation; Me, monomethylation. Charge, *m*/*z* and Mascot score are shown on the top right of each spectrum. All identified Siwi and Ago3 peptides are listed in Supplementary Table 1.

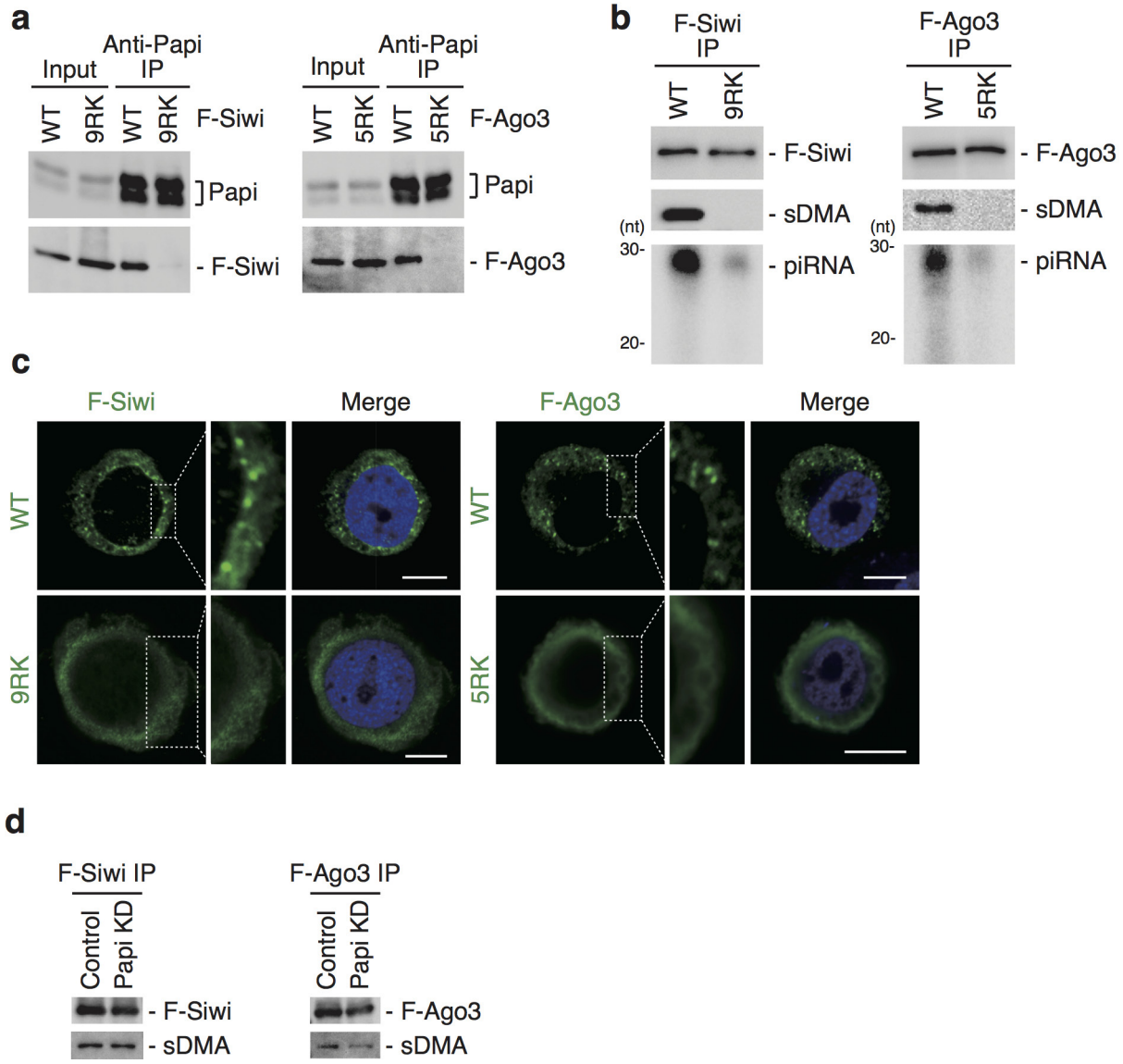

Extended Data Figure 4 | Analysis of Siwi and Ago3 mutants. a, Wild-type Flag–Siwi and Flag–Ago3, but not Flag–Siwi-9RK and Flag-Ago3-5RK mutants, are co-immunoprecipitated with Papi from BmN4 cells. **b**, Wild-type Flag–Siwi and Flag–Ago3, but not Flag–Siwi-9RK and Flag–Ago3-5RK mutants, are loaded with piRNAs in BmN4 cells. The middle (sDMA) shows that neither the Flag–Siwi-9RK nor Flag–Ago3-5RK mutant reacts with the Y12 antibody, which specifically recognizes sDMA. **c**, Wild-type Flag–Siwi and Flag–Ago3, but not Flag–Siwi-9RK and Flag–Ago3-5RK mutants, are localized to nuage in BmN4 cells (shown in green). Blue (DAPI staining) indicates the location of the nucleus. Scale bars, 10 μm. **d**, Papi depletion has little effect on sDMA modification of Flag–Siwi and Flag–Ago3 expressed in BmN4 cells.

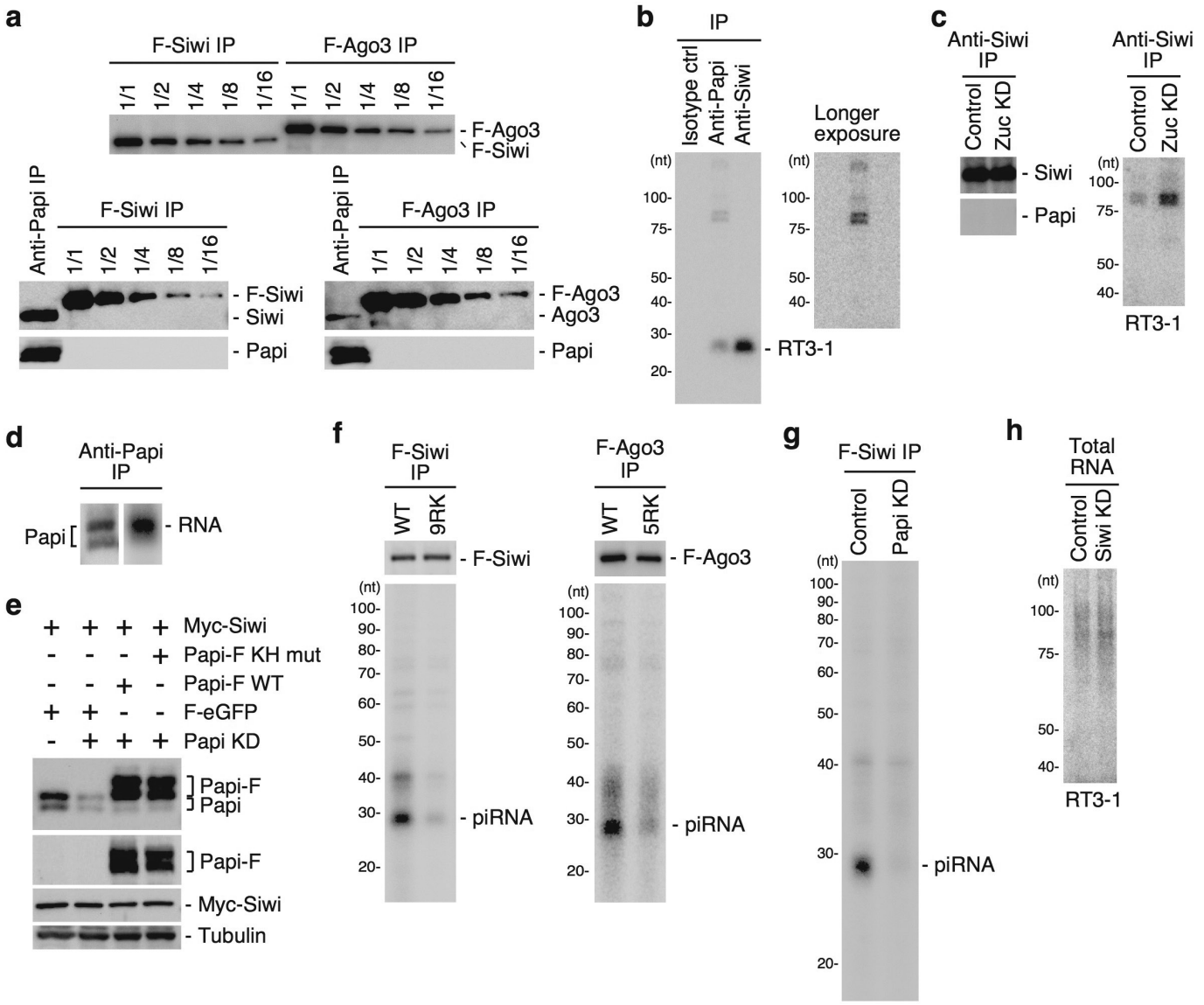

Extended Data Figure 5 | Papi complex analysis. a, Top, Flag–Siwi and Flag–Ago3 expressed in BmN4 cells were immunoisolated with anti-Flag antibody and probed with anti-Flag antibody after sequential dilution. Bottom, Flag–Siwi and Flag–Ago3 immunoisolated from BmN4 cells (the same samples as in the top panel) were probed with anti-Siwi and anti-Ago3 antibodies, respectively. Siwi and Ago3 co-immunoprecipitated with Papi were simultaneously probed with anti-Siwi and anti-Ago3 antibodies, respectively. The Papi complex was equally divided into two fractions and each fraction was used for each blot. Examination of the signal intensity revealed that the amount of Siwi within the Papi complex was approximately equal to 1/1.6 volume of Flag–Siwi and that the amount of Ago3 within the Papi complex was approximately equal to 1/16 volume of Flag–Ago3. Comparison of the signal intensity on the top and bottom blots suggests that the ratio of abundance of Siwi and Ago3 in the Papi complex is 10:1. **b**, Northern blotting shows that the Papi complex contains RT3-1 int-piRNAs. **c**, Northern blotting shows that Siwi in a form associated with Papi on mitochondria binds RT3-1 int-piRNAs independently of Papi. The Siwi–int-piRNA association is maintained even after Zuc depletion. **d**, CLIP analysis shows that only the long form, but not the short form, of endogenous Papi in BmN4 cells interacts with RNA *in vivo*. **e**, Western blotting using anti-Papi (top) and anti-Flag (second from the top) antibodies shows that wild-type Papi–Flag and the KH mutant are equally expressed in BmN4 cells, in which endogenous Papi has been depleted by RNAi. Western blotting using anti-Myc (third from the top) shows that the levels of Myc–Siwi are approximately equal in the cells. Tubulin was used as a loading control (bottom). Both wild-type Papi–Flag and the KH mutant were mutated to be RNAi resistant. **f**, Flag–Siwi-9RK and Flag–Ago3-5RK mutants bind with little int-piRNA. **g**, Flag–Siwi binds with little int-piRNA in Papi-lacking BmN4 cells. **h**, Northern blotting shows that int-piRNAs are still present in Siwi-depleted BmN4 cells.

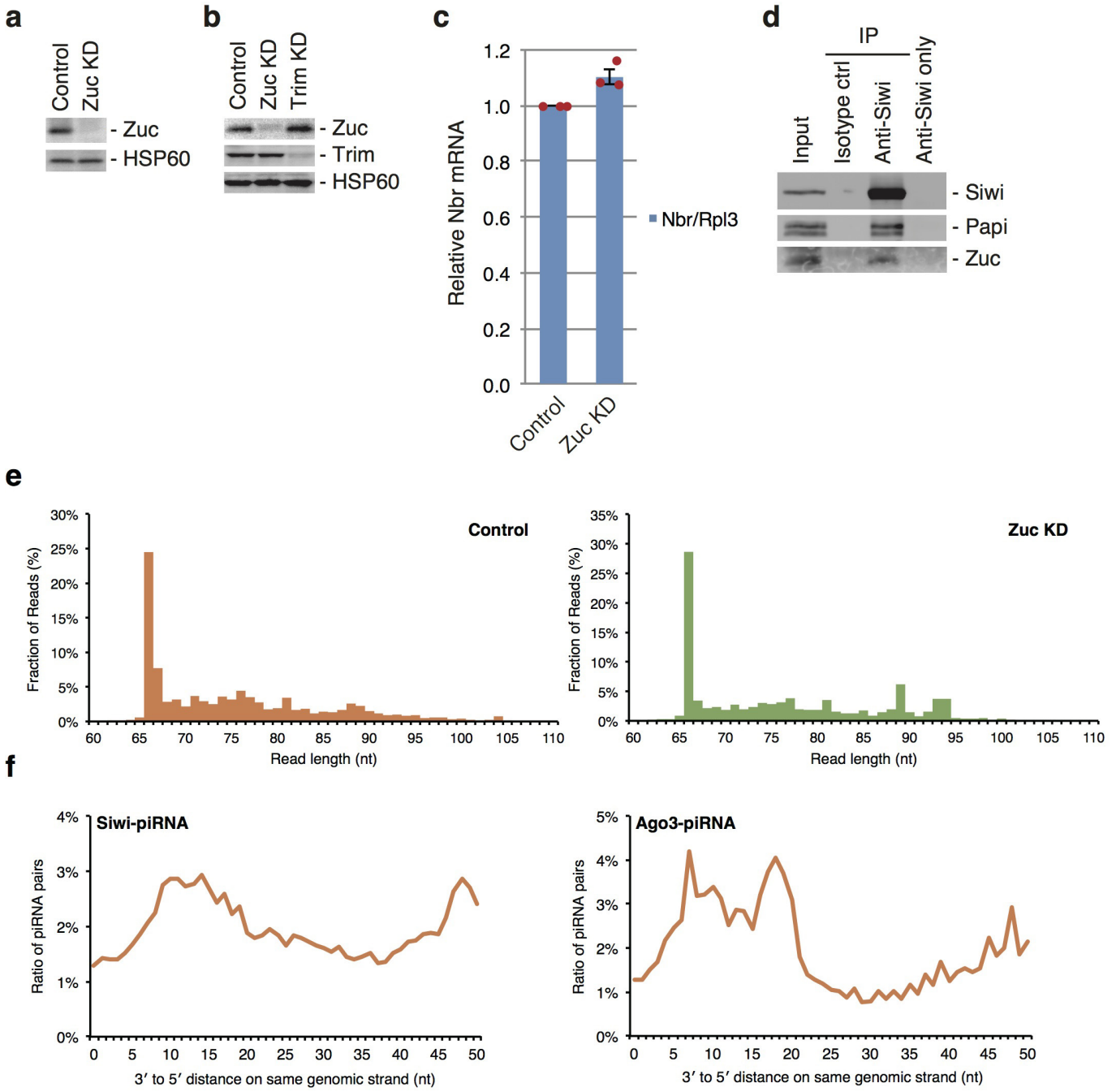

Extended Data Figure 6 | RNAi efficiency, Siwi–Papi–Zuc interaction and analysis of Papi-associated intermediates and piRNA phasing. **a**, Western blotting shows that Zuc is efficiently depleted by RNAi. HSP60 is used as a loading control. **b**, Western blotting shows that Zuc and Trim are efficiently depleted by RNAi. Zuc and Trim depletion had little effect on the protein levels of Trim and Zuc, respectively. HSP60 is shown as a loading control. **c**, qRT–PCR shows that the level of *Nbr* is not affected by Zuc depletion in BmN4 cells. Data are mean ± s.e.m. of three independent experiments. **d**, Zuc and Papi are detected in the Siwi complex immunoisolated from the mitochondrial fraction of BmN4 cells. **e**, The size distribution of Papi-associated intermediates mapped to transposons. **f**, Analyses of phased piRNAs in Papi-associated intermediates. The distance between the 3′ end of the upstream piRNA and the 5′ end of the downstream piRNA on the same genomic strand is analysed.

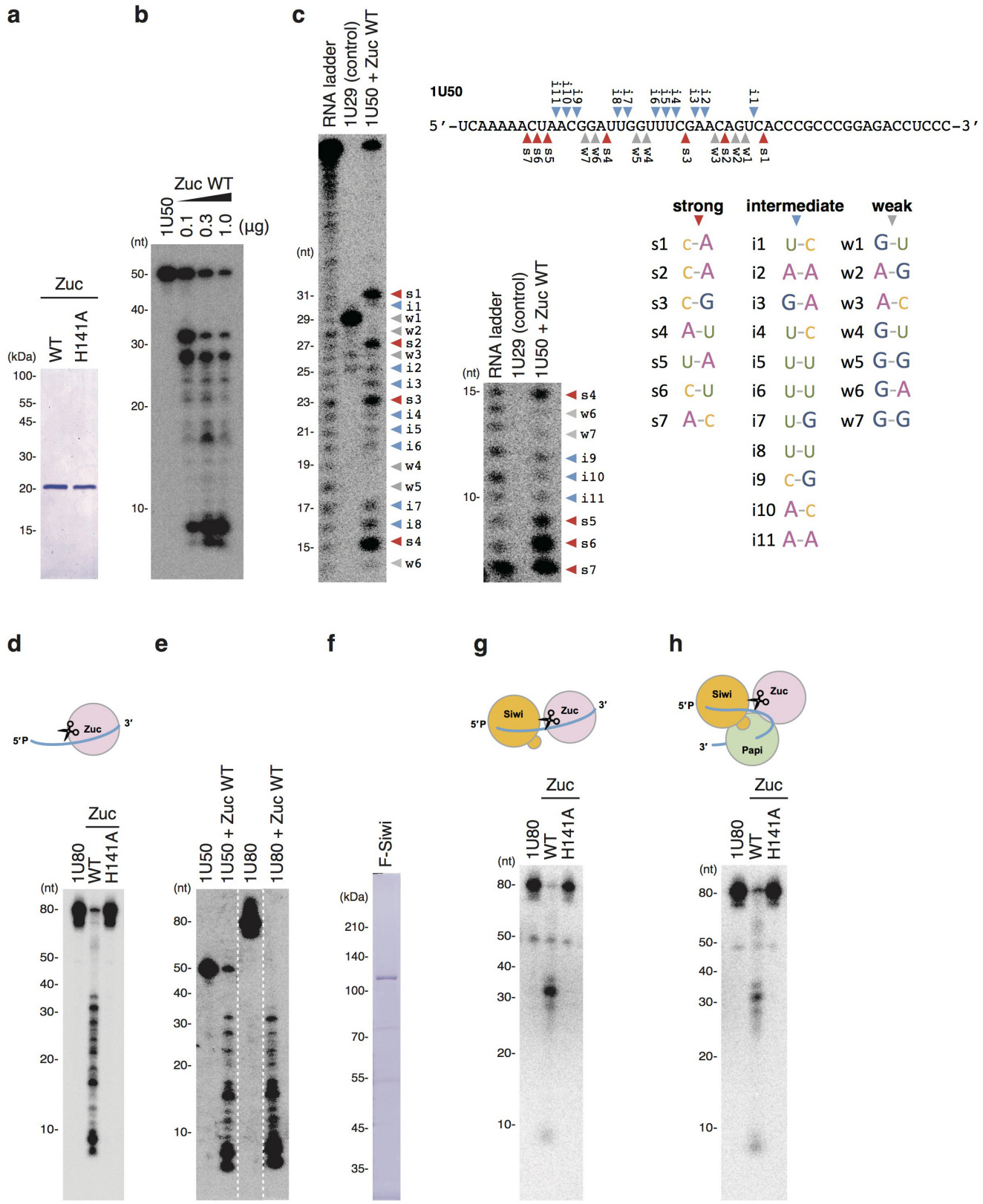

Extended Data Figure 7 | Analyses of Zuc RNA cleavage. a, Coomassie brilliant blue (CBB)-stained gel showing purified wild-type Zuc and the Zuc(H141A) mutant. **b**, Wild-type Zuc in **a** cleaves 1U50 in a dose-dependent manner. **c**, Detailed analyses of Zuc RNA cleavage. The left gel shows RNA ladders ranging from 14 to 50 nucleotides. The right gel shows RNA ladders ranging from 7 to 15 nucleotides. Relatively 'strong' RNA bands are indicated by red arrowheads (s1–s7). 'Intermediate' RNA bands are indicated by blue arrowheads (i1–i11). Relatively 'weak' RNA bands are indicated by grey arrowheads (w1–w7). 1U29 is an authentic RNA, the sequence of which is identical to that of 1U50 RNA over 1–29 nucleotides from the 5′ end. Classification of strong, intermediate and weak RNA bands is carried out in accordance with the intensity of each band. **d**, An 80-nucleotide RNA, 1U80, is cleaved by wild-type Zuc. **e**, Cleavage patterns of 1U50 and 1U80 by wild-type Zuc are compared. **f**, CBB-stained gel showing purified Flag–Siwi. **g**, 1U80 pre-loaded onto Flag-Siwi in **f** is cleaved by wild-type Zuc. **h**, The Siwi–1U80 RNA complex was first incubated with Papi, which was immunopurified using an anti-Papi antibody, and then treated with wild-type Zuc.

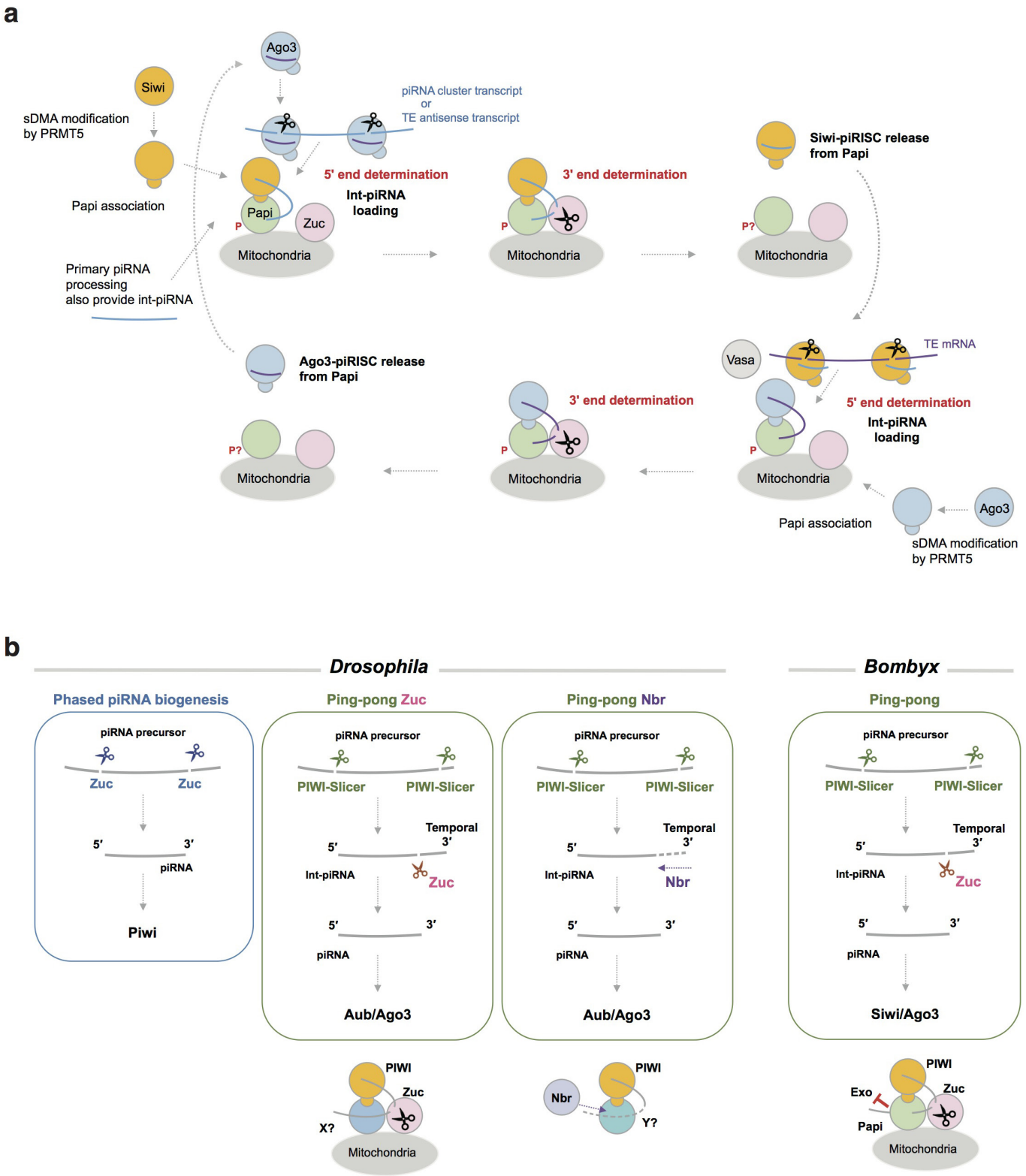

Extended Data Figure 8 | A new model for piRNA biogenesis in *Bombyx*. **a**, A model for the ping-pong cycle in *Bombyx*. Papi is localized on the surface of mitochondria through MLS, whereas KH domains are required for Papi to exhibit RNA-binding activity. The Papi Tudor domain and sDMA modification of Siwi and Ago3 are required for the Siwi–Papi and Ago3–Papi interactions. It remains unclear how Papi is maintained in an RNA-free state before the Papi–PIWI association. Also, it remains unclear how piRISC upon its formation is displaced from Papi, and how piRISC avoids re-association with Papi. Conformational change of piRISC may be involved. **b**, *Drosophila* phased piRNA biogenesis involves Zuc–Zuc endonucleolytic cleavage for piRNA 5′ and 3′ end formation. PIWI-slicer-Nbr exonucleolytic trimming and PIWI-slicer-Zuc endonucleolytic cleavage produce piRNAs in the ping-pong cycle. The role of *Drosophila* Papi remains under discussion. Its functional homologue(s) (shown as X and Y) may function with Zuc and Nbr. *Bombyx* lacks a gene homologue of *Drosophila* Piwi, so it does not have to accommodate phased piRNA biogenesis. Because of this, Zuc endonuclease might not be used for piRNA 5′ end formation. However, PIWI-slicer-Zuc endonucleolytic cleavage produces piRNAs in the ping-pong cycle. We infer that the 3′-to-5′ exonuclease cannot trim the 3′ end of the intermediate because Papi impedes this reaction. This model shows that *Bombyx* piRNAs are produced in a manner that depends on PIWI-slicer and Zuc. There may also be alternative pathways that have less of an effect on the overall levels of piRNA production.

nature research

Corresponding author(s): Mikiko C. Siomi

☐ Initial submission ☐ Revised version ☒ Final submission

Life Sciences Reporting Summary

Nature Research wishes to improve the reproducibility of the work that we publish. This form is intended for publication with all accepted life science papers and provides structure for consistency and transparency in reporting. Every life science submission will use this form; some list items might not apply to an individual manuscript, but all fields must be completed for clarity.

For further information on the points included in this form, see Reporting Life Sciences Research. For further information on Nature Research policies, including our data availability policy, see Authors & Referees and the Editorial Policy Checklist.

Experimental design

1. Sample size

Describe how sample size was determined.

Not applicable

2. Data exclusions

Describe any data exclusions.

We had one data as "data not shown" in the manuscript.

The predicted structures of 80-nt and 50-nt RNAs are not similar to each other (page14): Because we thought that it was not crucial to show. However, we are happy to show the data upon request.

3. Replication

Describe whether the experimental findings were reliably reproduced.

All attempts at replication were successful.

4. Randomization

Describe how samples/organisms/participants were allocated into experimental groups.

Not applicable

5. Blinding

Describe whether the investigators were blinded to group allocation during data collection and/or analysis.

Not applicable

Note: all studies involving animals and/or human research participants must disclose whether blinding and randomization were used.

6. Statistical parameters

For all figures and tables that use statistical methods, confirm that the following items are present in relevant figure legends (or in the Methods section if additional space is needed).

n/a	Confirmed
☒	☐ The exact sample size (*n*) for each experimental group/condition, given as a discrete number and unit of measurement (animals, litters, cultures, etc.)
☐	☒ A description of how samples were collected, noting whether measurements were taken from distinct samples or whether the same sample was measured repeatedly
☐	☒ A statement indicating how many times each experiment was replicated
☒	☐ The statistical test(s) used and whether they are one- or two-sided (note: only common tests should be described solely by name; more complex techniques should be described in the Methods section)
☒	☐ A description of any assumptions or corrections, such as an adjustment for multiple comparisons
☒	☐ The test results (e.g. *P* values) given as exact values whenever possible and with confidence intervals noted
☐	☒ A clear description of statistics including central tendency (e.g. median, mean) and variation (e.g. standard deviation, interquartile range)
☐	☒ Clearly defined error bars

See the web collection on statistics for biologists for further resources and guidance.

Software

Policy information about availability of computer code

7. Software

Describe the software used to analyze the data in this study.	For analyzing the reads obtained from deep sequencing analysis, cutadapt, Bowtie, motifStack from R package, and in-house script for calculation of the distance between intermediates and piRNA-phasing analysis (which is available upon request), were used.

For manuscripts utilizing custom algorithms or software that are central to the paper but not yet described in the published literature, software must be made available to editors and reviewers upon request. We strongly encourage code deposition in a community repository (e.g. GitHub). *Nature Methods* guidance for providing algorithms and software for publication provides further information on this topic.

Materials and reagents

Policy information about availability of materials

8. Materials availability

Indicate whether there are restrictions on availability of unique materials or if these materials are only available for distribution by a for-profit company.	No unique materials were used.

9. Antibodies

Describe the antibodies used and how they were validated for use in the system under study (i.e. assay and species).	Anti-Siwi, Ago3, PAPI, Zuc and Trim antibodies were produced from immunized mouse, respectively. Anti-myc (catalog number: C3956), Anti-HSP60 (catalog number: SMC-110B), Anti-DDDDK-tag (Anti-Flag antibody) (catalog number: FLA-1) and anti-Tubulin antibodies (catalog number: E7) were purchased from Sigma, StressMarq Biosciences, MLB and DSHB, respectively. Y12 antibody was gifted from Dr. Gideon Dreyfuss.

10. Eukaryotic cell lines

a. State the source of each eukaryotic cell line used.	BmN4 cells were gifted from National Institute of Agrobiological Sciences (NIAS).
b. Describe the method of cell line authentication used.	We think that BmN4 cells used have been authenticated, because BmN4 were gifted from NIAS.
c. Report whether the cell lines were tested for mycoplasma contamination.	BmN4 cells were not tested for mycoplasma contamination.
d. If any of the cell lines used are listed in the database of commonly misidentified cell lines maintained by ICLAC, provide a scientific rationale for their use.	BmN4 cells are not misidentified cell lines.

Animals and human research participants

Policy information about studies involving animals; when reporting animal research, follow the ARRIVE guidelines

11. Description of research animals

Provide details on animals and/or animal-derived materials used in the study.	No applicable

Policy information about studies involving human research participants

12. Description of human research participants

Describe the covariate-relevant population characteristics of the human research participants.	No applicable